

## Metal-free Catalysis | Very Important Paper |

SPECIAL  
ISSUE

## Cyclodextrin-based Mesoporous N-Doped Carbon Hybrids with High Heterocatalytic Activity

Jun Tian,<sup>[a]</sup> Yong Chen,<sup>[a]</sup> Wei Li,<sup>[b]</sup> Yu-Ping Liu,<sup>[c]</sup> Wei-Lei Zhou,<sup>[a]</sup> and Yu Liu<sup>\*,[a, d]</sup>

**Abstract:** A convenient approach for the construction of nitrogen-doped mesoporous carbon material from native cyclic oligosaccharide  $\beta$ -cyclodextrin and N-containing small molecules was established. The resultant N-doped carbon hybrids, which possessed high Brunauer–Emmett–Teller (BET) surface area as well as appropriate pore volumes and pore diameters, could serve as highly efficient metal-free heterocatalysts with very good catalytic activity as well as generality and could be easily recovered without any compromise of catalytic performance.

Functional mesoporous carbon materials have attracted much attention in recent years and are widely employed for energy storage, separation technologies, and electrochemistry owing to their large specific surface areas, adjustable pore size, excellent stability and conductivity.<sup>[1]</sup> However, as an efficient catalyst, appropriate and sufficient active sites are also required in addition to these outstanding features.<sup>[2]</sup> Therefore, heteroatoms, especially nitrogen atoms, were incorporated into the carbon matrix to improve the catalytic performance of active sites or to directly serve as active sites for corresponding reactions.<sup>[3]</sup> Recently, nitrogen-doped carbon materials were widely reported as supports for metals or their oxides in various reac-

tions including oxidation,<sup>[4]</sup> dehydrogenation,<sup>[5]</sup> hydrogenation,<sup>[6]</sup> hydrochlorination,<sup>[7]</sup> Fischer–Tropsch synthesis,<sup>[8]</sup> and the decomposition of toxic chemicals,<sup>[9]</sup> and the incorporation of nitrogen atoms significantly enhanced the catalytic activity of these metals or their oxides. However, the high price and the possible contamination of metal catalysts greatly limited their applications. Therefore, metal-free catalysis is undoubtedly regarded as an effective method to solve the above-mentioned problems.<sup>[10]</sup> For example, Arai et al.<sup>[11]</sup> prepared various activated carbons containing nitrogen for the aerobic oxidation of alcohols. Similarly, the oxygen reduction reaction could also be carried out by using nitrogen-doped carbon materials.<sup>[12]</sup> Ma et al.<sup>[13]</sup> and Song et al.<sup>[14]</sup> reported nitrogen-incorporated carbon materials for the selective oxidation of ethylbenzene to acetophenone. Moreover, Bao et al.<sup>[15]</sup> used a nitrogen-incorporated carbon as a substitute for mercury in the catalytic hydrochlorination of acetylene. Clearly, the design and fabrication of nitrogen-doped carbon material for the synthesis of some important chemical intermediates was meaningful.

Herein, we consciously employed  $\beta$ -cyclodextrin ( $\beta$ -CD), a kind of cyclic oligosaccharide composed of seven D-glucopyranoside units, and N-containing small molecules, that is, melamine, dicyandiamide, and guanidine sulfamate, to construct a series of novel nitrogen-doped mesoporous carbon materials that possess high Brunauer–Emmett–Teller (BET) surface area ( $494.6\text{--}1307.2\text{ m}^2\text{ g}^{-1}$ ) as well as appropriate pore volumes ( $0.43\text{--}2.36\text{ cm}^3\text{ g}^{-1}$ ) and pore diameters ( $3.45\text{--}7.22\text{ nm}$ ). Significantly, the selected material exhibited a very good catalytic performance for the hydrogenation of 4-nitroethylbenzene to 4-ethylaniline (conversion  $>99.9\%$ , selectivity  $>99.9\%$ ) as well as a fairly excellent generality for the hydrogenation of various nitroarenes (conversion  $>99.9\%$ , selectivity  $>92.5\%$ ) and could be easily recovered by centrifugation without any compromise of catalytic performance.

Figure 1 illustrates the two construction routes of N-doped mesoporous carbon hybrids. In the first route,  $\beta$ -CD was subsequently pre-treated with  $\text{H}_2\text{SO}_4$  and the ordered mesoporous silica SBA-15 in the absence or presence of N-containing small molecules, followed by the calcination and removal of the silica template, to give carbon hybrids named OMC (ordered mesoporous carbon constructed from  $\beta$ -CD only), NOMC-D (N-doped ordered mesoporous carbon constructed from  $\beta$ -CD and dicyandiamide), NOMC-T (N-doped ordered mesoporous carbon constructed from  $\beta$ -CD and melamine), and NOMC-G (N-doped ordered mesoporous carbon constructed from  $\beta$ -CD and guanidine sulfamate). In another route, tetraethoxysilane

[a] J. Tian, Prof. Y. Chen, W.-L. Zhou, Prof. Y. Liu  
College of Chemistry, State Key Laboratory of Elemento-Organic Chemistry  
Nankai University  
Tianjin 300071 (P. R. China)  
E-mail: yuliu@nankai.edu.cn

[b] Prof. W. Li  
College of Chemistry, Key Laboratory of Advanced Energy Materials Chemistry (Ministry of Education)  
Nankai University  
Tianjin 300071 (P. R. China)

[c] Prof. Y.-P. Liu  
Research Center for Analytical Sciences  
Nankai University  
Tianjin 300071 (P. R. China)

[d] Prof. Y. Liu  
Collaborative Innovation Center of Chemical Science and Engineering (Tianjin)  
Nankai University  
Tianjin 300071 (P. R. China)

Supporting information for this article can be found under:  
<https://doi.org/10.1002/ajoc.201700155>.

This manuscript is part of the Board Members special issue celebrating the 5<sup>th</sup> anniversary and the success of Asian Journal of Organic Chemistry. Click here to see the Table of Contents of the special issue.

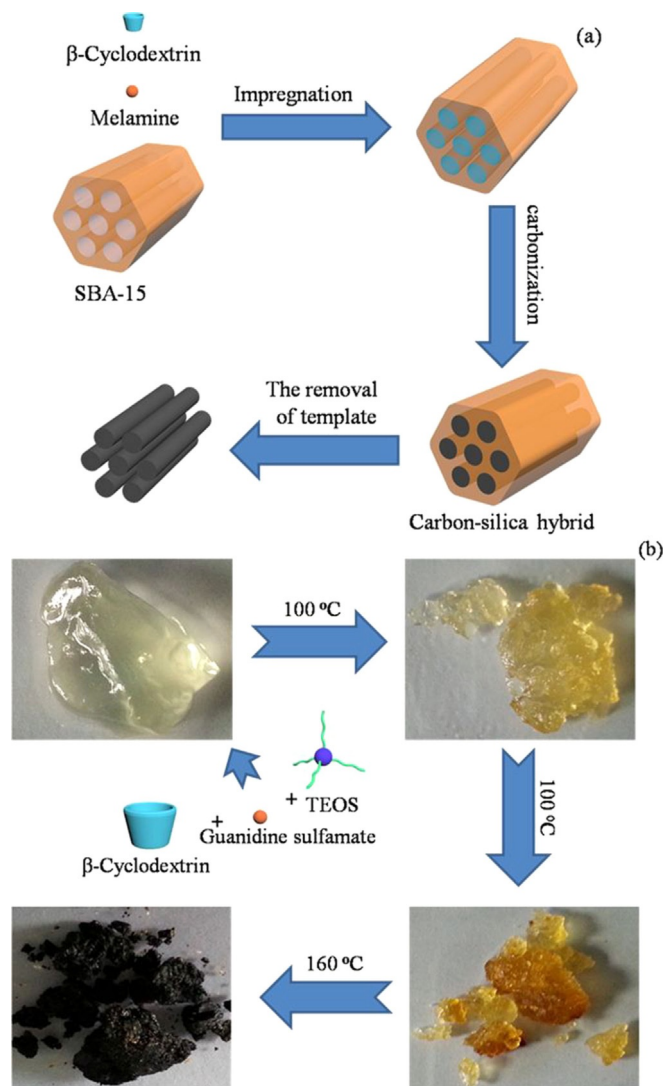
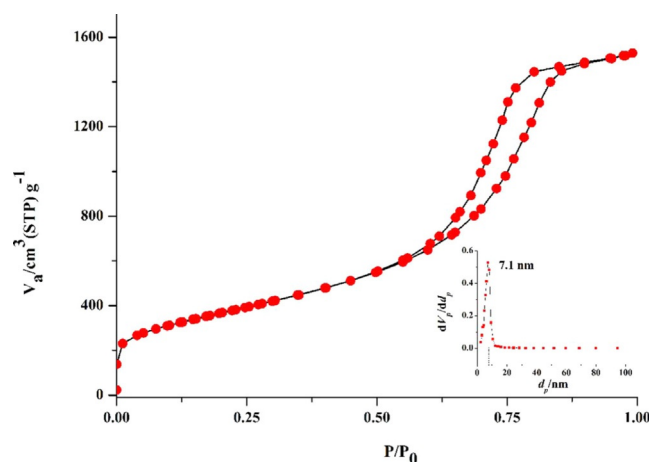


**Figure 1.** Construction of nitrogen-doped mesoporous carbon materials from  $\beta$ -CD without (a) and with (b) a gelation process.

(TEOS) was used as a template instead of SBA-15, and its reaction with  $\beta$ -CD, guanidine sulfamate, and  $\text{H}_2\text{SO}_4$  gave a pale yellow and transparent carbon-silica hybrid gel, which was converted to the N-doped ordered mesoporous carbon named Gel-NMC through the calcination and the subsequent removal of silica template (Table 1).

Figure 2 clearly shows the  $\text{N}_2$  absorption-desorption isotherm curve and the pore diameter distribution of Gel-NMC, which displayed a typical type IV isotherm curve with a hysteresis loop and a narrow pore diameter distribution at a maximum of approximately 7.1 nm, indicating the Gel-NMC should be a mesoporous material.<sup>[16]</sup> Similar  $\text{N}_2$  absorption-desorption isotherm curves were also observed in the cases of OMC, NOMC-D, NOMC-T, and NOMC-G (see the Supporting Information). The BET surface area, pore volume, and average pore diameter of the obtained carbon hybrids are provided in Table 2. As seen in Table 2, OMC gave a high BET surface area ( $989.2 \text{ m}^2 \text{ g}^{-1}$ ), a large pore volume ( $0.91 \text{ cm}^3 \text{ g}^{-1}$ ), and a moder-

Table 1. Structural and textural properties of as-prepared carbon materials.			
Material	BET surface area [ $\text{m}^2 \text{ g}^{-1}$ ]	Pore volume [ $\text{cm}^3 \text{ g}^{-1}$ ]	Average pore diameter [nm]
OMC	$989.2 \pm 0.20$	$0.91 \pm 0.025$	$3.69 \pm 0.030$
NOMC-D	$494.6 \pm 0.14$	$0.43 \pm 0.020$	$3.45 \pm 0.014$
NOMC-T	$818.7 \pm 0.33$	$0.79 \pm 0.037$	$3.56 \pm 0.028$
NOMC-G	$919.6 \pm 0.21$	$0.82 \pm 0.024$	$3.58 \pm 0.012$
Gel-NMC	$1307.2 \pm 0.15$	$2.36 \pm 0.018$	$7.22 \pm 0.023$



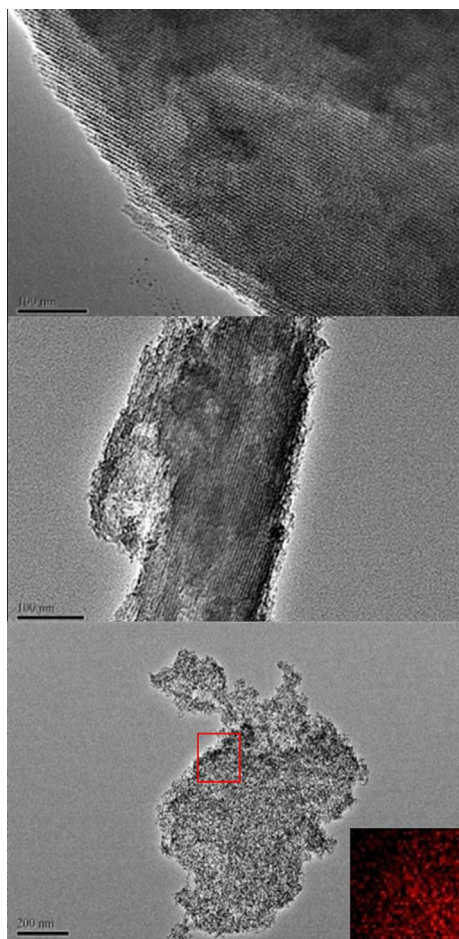
**Figure 2.** Nitrogen absorption-desorption isotherm of Gel-NMC. Inset: Barrett-Joyner-Halenda (BJH) pore size distribution obtained from the adsorption branch.

Table 2. Nitrogen contents, $I_D/I_G$ , and $G_N/P_N$ values of carbon materials.				
Materials	TNC <sup>[a]</sup> [%]	SNC <sup>[b]</sup> [%]	$I_D/I_G$	$G_N/P_N$ <sup>[c]</sup>
OMC	–	–	$2.16 \pm 0.02$	–
NOMC-D	$1.58 \pm 0.04$	trace	$2.32 \pm 0.03$	1.15
NOMC-T	$2.46 \pm 0.08$	0.79	$2.15 \pm 0.02$	1.55
NOMC-G	$1.67 \pm 0.02$	trace	$2.11 \pm 0.01$	1.36
Gel-NMC	$6.07 \pm 0.03$	6.52	$2.63 \pm 0.02$	1.49

[a] The total nitrogen contents obtained by elemental analysis. [b] The nitrogen content on the surface of materials obtained by XPS. [c] The relative ratio of graphitic N and pyridinic N obtained by the ratio of the corresponding areas in XPS.

ate average pore diameter (3.69 nm). After the nitrogen atoms were incorporated, the obtained NOMCs gave decreased BET surface areas, pore volumes, and average pore diameters, which might be attributed to the expansion of the carbon wall.<sup>[17]</sup> However, Gel-NMC gave a 1.3–2.6 times higher BET surface area, a 2.6–5.5 times higher pore volume, and a 1.9–2.1 times higher average pore diameter than that of OMC or NOMCs, suggesting that the pyrolysis of guanidine sulfamate wrapped in the carbon-silica hybrid gel would lead to the formation of new pore structures.

The morphology of obtained carbon hybrids was investigated by TEM. As seen in Figure 3 a–b, TEM images of either OMC



**Figure 3.** TEM images for OMC (a), NOMC-G (b), and Gel-NMC (c). Inset: N mapping for Gel-NMC.

or NOMC-G showed a number of ordered porous structures originating from the removal of ordered mesoporous silica SBA-15. Moreover, the order degree of NOMC-G was clearly less than those of OMC, which was in accord with the results of XRD (Figure S2a in the Supporting Information). However, there exist a large amount of wormhole-like mesopores in the TEM image of Gel-NMC (Figure 3c). The formation of these mesopores might be due to the pyrolysis of guanidine sulfamate and the removal of the silica template. During the carbonization of the carbon-silica hybrid, the inserted guanidine sulfamate might decompose and re-construct into graphitic N, pyrrole N, pyridinic N, or pyridine N oxide. The formation of these types of nitrogen atoms could effectively improve the catalytic performance of the carbon matrix. The distribution of elemental nitrogen could be displayed by nitrogen elemental mapping. As revealed in Figure 3c (inset), the elemental nitrogen was uniformly doped into the structure of Gel-NMC.

Elemental analysis and X-ray photoelectron spectroscopy (XPS) of NOMCs and Gel-NMC were further performed to investigate the oxygen species, nitrogen type, and nitrogen content on the surface or in the bulk phase of these porous N-doped carbon materials. As seen in Figures S3–S4 (in the Supporting Information) and Table 2, the nitrogen content of NOMCs ob-

tained from elemental analysis results are always much higher than the corresponding values obtained from the N1s signal at approximately 400 eV in the XPS spectra (Figure S3a in the Supporting Information), indicating that the majority of nitrogen atoms may be distributed in the bulk phase of NOMCs. However, the nitrogen content (6.07%) of Gel-NMC obtained from elemental analysis results was almost the same as that from XPS results (6.52%), indicating that the doped nitrogen elemental was uniformly distributed in the structure of Gel-NMC, which was consistent with the nitrogen elemental mapping results. Moreover, the N1s spectra of NOMCs (Figure S3b–d in the Supporting Information) showed two clear signals assigned to the pyridinic N (ca. 398 eV) and the graphitic N (ca. 401 eV),<sup>[18]</sup> and NOMC-T gave the highest ratio between the graphitic N and the pyridinic N ( $G_N/P_N=1.55$ ) among the examined NOMCs. A possible reason might be that most of the melamine might directly convert to the graphitic N at elevated temperature.<sup>[19]</sup> In contrast, the N1s spectra of Gel-NMC (Figure S3f in the Supporting Information) exhibited three signals assigned to the pyridinic N (ca. 398 eV), the graphitic N (ca. 401 eV), and the pyridine N oxide (ca. 406 eV). Moreover, the O1s spectra (Figure S4 in the Supporting Information) of these three carbon materials all exhibited one signal at approximately 533 eV. The existence of this oxygen species would lead to the formation of defects or edges in the carbon skeleton.

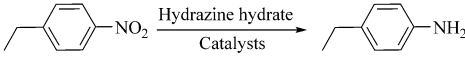
As illustrated in the wide-angle XRD patterns (Figure S2b in the Supporting Information), each of carbon materials presented two diffraction peaks at  $2\theta=23.1^\circ$  and  $43.7^\circ$ , which were ascribed to the diffraction of the (002) plane and (101) plane, respectively. This phenomenon demonstrated the formation of the graphitic structure within the carbon skeleton of OMC, NOMCs, or Gel-NMC.<sup>[20]</sup> In addition, the formation of graphitic structure was also confirmed by Raman spectroscopy. As shown in Figure S5 (in the Supporting Information), the Raman spectra of OMC, NOMCs, or Gel-NMC all displayed two bands at around  $1590\text{ cm}^{-1}$  and  $1350\text{ cm}^{-1}$ , assigned to the G band and D band of the graphitic skeleton, respectively. Generally, the G band always refers to the planar vibration of  $sp^2$  carbon atoms in the graphitic layer, and the D band refers to the structural defects as well as the disordered structures at the edge of graphitic layers. Therefore, the distribution of defects or edges on the graphitic walls could be determined by the area ratio ( $I_D/I_G$ ) between the D band and G band. As shown in Table 2, all of the examined carbon materials gave relatively high  $I_D/I_G$  values ( $>2.0$ ), indicating that there exist a number of defects or edges in the graphitic structure of these carbon materials. It is noteworthy that these defects or edge parts possess a unique electronic state in the carbon matrix and thus could interact with heteroatomic groups including OH,  $\text{NO}_2$ , and halogen, leading to the activation of heteroatomic groups and the promotion of catalytic activity of carbon materials to some extent. In addition, the thermogravimetric (TG) profile (Figure S6 in the Supporting Information) of OMC showed clear weight losses above  $500^\circ\text{C}$ , referring to the collapse of the skeleton structure. The TG profiles of NOMC-G and Gel-NMC displayed lower weight-loss temperatures than that of



OMC, originating from the increase of defects or edges in the graphitic structure of these carbon materials.

It is well known that aromatic amines are very important chemical intermediates for the manufacture of pharmaceuticals, agrochemicals, dyes, and fine chemicals, and the most commonly used method for the synthesis of aromatic amines is the reduction of nitroaromatic compounds.<sup>[21]</sup> Herein, the catalytic activity of these carbon materials for the nitroarene hydrogenation reaction was investigated (Table 3). Without the

**Table 3.** The catalytic activity of different carbon materials for hydrogenation reactions.<sup>[a]</sup>

				
Catalyst	$T^{[b]}$ [°C]	$t$ [h]	Conv. <sup>[c]</sup> [%]	Sel. <sup>[d]</sup> [%]
None	100	12	1.1 ± 0.2	> 99.9
Active carbon	100	12	21.4 ± 0.1	> 99.9
OMC	100	12	65.9 ± 0.1	> 99.9
NOMC-D	100	12	72.7 ± 0.2	> 99.9
NOMC-T	100	12	> 99.9	99.9 ± 0.1
NOMC-G	90	7.5	> 99.9	99.2 ± 0.1
Gel-NMC	90	7.5	> 99.9	> 99.9

[a] Reaction conditions: 0.076 g 4-nitroethylbenzene, 0.15 g hydrazine hydrate, 5 mg catalyst, 2 mL ethanol. [b] Reaction temperature. [c] The conversion of 4-nitroethylbenzene. [d] The selectivity of 4-ethylaniline.

catalyst, the reaction of 4-nitroethylbenzene with hydrazine hydrate gave a very low conversion of 1.1% at 100 °C for 12 h, and this conversion could increase to 21.4% in the presence of amorphous active carbon as a catalyst. The application of OMC as a catalyst instead of active carbon could efficiently increase the conversion to 65.9%, because OMC could provide ordered pore structures with the appropriate size as reaction sites for 4-nitroethylbenzene and hydrazine. Significantly, after the nitrogen atoms were doped into OMC, the obtained catalyst NOMC-T further promoted the nitroarene hydrogenation reaction to a ultrahigh conversion of up to > 99.9%, accompanied by a high selectivity of up to > 99.9%. More interestingly, the application of NOMC-G or Gel-NMC could give the same results (conversion > 99.9%, selectivity > 99.0%) at a lower temperature and a shorter reaction time. A possible catalytic mechanism is illustrated in Figure 4. Therein, the incorporated graphitic N atoms with positive charges would interact with the terminal oxygen atoms of 4-nitroethylbenzene. Moreover, the pyridinic N atoms could change the electronic structure of defects or edges in the carbon matrix, especially the adjacent carbon atoms, which subsequently activated the 4-nitroethylbenzene and promoted the conversion of 4-nitroethylbenzene to 4-ethylaniline.

In addition, the hydrogenation of various nitroaromatics was carried out to evaluate the generality of Gel-NMC. As shown in Table S1 (in the Supporting Information), a > 99.9% conversion and a > 92.5% selectivity could be obtained for all examined hydrogenation reactions, indicating the excellent generality of

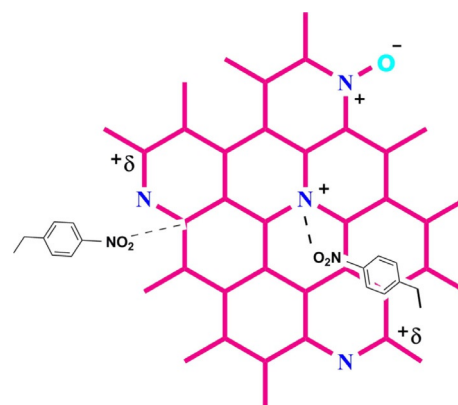


**Figure 4.** The possible interaction mechanism of carbon material with 4-nitroethylbenzene.

Gel-NMC. Significantly, 2-amino-4-chlorophenol, the key intermediate in the manufacture of chlorzoxazone (a centrally acting muscle relaxant drug), could be efficiently obtained by using Gel-NMC instead of the commonly used Fe-based catalyst. Moreover, Gel-NMC could be easily recovered from the reaction system by centrifugation and reused at least five times without any deactivation (Figure 5).

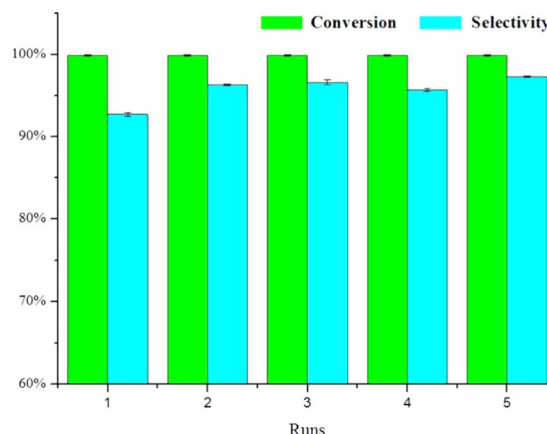


**Figure 5.** Recovery and reuse of Gel-NMC as a catalyst for the hydrogenation of 2-nitro-4-chlorophenol.

In summary, we employed  $\beta$ -CD and N-containing small molecules to construct a series of novel N-doped mesoporous carbon materials by a convenient approach. With a high BET surface area, appropriate pore volume and pore diameter, these carbon materials could be applied in the highly efficient catalysis of nitroarene hydrogenation reactions, giving very high conversions for various nitroarene substrates. We believe that the judicious selection of cyclodextrins and nitrogen sources will continue to energize and expend the exciting potentials of these N-doped carbon hybrids in other fields of catalytic chemistry.

## Experimental Section

### Preparation of materials

The ordered mesoporous silica SBA-15 was prepared according to a reference method.<sup>[22]</sup> Pluronic 123 ( $\text{EO}_{20}\text{PO}_{70}\text{EO}_{20}$ ,  $M_w=5800$ , 4.0 g) was dissolved in HCl (152 mL,  $1.6 \text{ mol L}^{-1}$ ) solution under vigorous stirring. The solution was heated to  $35^\circ\text{C}$ , and then tetraethoxysilane (TEOS, 8.8 g) was added. The mixture was kept at  $35^\circ\text{C}$  for 24 h under static conditions and then transferred into a hydrothermal kettle and aged at  $100^\circ\text{C}$  for another 24 h. The product was filtered, dried without washing, and calcined at  $550^\circ\text{C}$  for 4 h. The ordered mesoporous carbon (OMC) was prepared as follows.<sup>[23]</sup>  $\beta$ -CD (1.25 g) was added to aqueous  $\text{H}_2\text{SO}_4$  (2.7 wt%, 5.14 g) solution at room temperature under vigorous stirring. Subsequently, the suspension was heated to  $100^\circ\text{C}$ , and SBA-15 (1.0 g) was added. After being stirred for 6 h, the temperature was increased to  $160^\circ\text{C}$ , and the reaction mixture was kept at this temperature for another 6 h. To this silica sample containing partially polymerized or carbonized  $\beta$ -CD, a mixture of  $\beta$ -CD (0.80 g),  $\text{H}_2\text{SO}_4$  (0.09 g), and  $\text{H}_2\text{O}$  (5 g) was added, and the suspension was stirred at  $100^\circ\text{C}$  for 6 h and then heated to  $160^\circ\text{C}$  for another 6 h. The complete calcination was carried out in a tubular furnace at  $600^\circ\text{C}$  for 3 h and then at  $900^\circ\text{C}$  for 4 h under  $\text{N}_2$ . The heating rates were  $1^\circ\text{C min}^{-1}$  below  $600^\circ\text{C}$  and  $5^\circ\text{C min}^{-1}$  above  $600^\circ\text{C}$ . This carbon-silica composite was further treated twice by heating at reflux in NaOH solution (10 mL,  $1 \text{ mol L}^{-1}$  in 1:1 ethanol/ $\text{H}_2\text{O}$ ) for 2 h to remove the silica template. The template-free product was collected by filtration, washed with water to neutral (pH 7.0), and dried at  $80^\circ\text{C}$  for 24 h.

The N-doped ordered mesoporous carbon (NOMC) was constructed by a similar process to that of OMC in the presence of different nitrogen sources. That is,  $\beta$ -CD (1.14 g) and nitrogen sources including melamine, dicyandiamide, or guanidine sulfamate (0.11 g) were added into  $\text{H}_2\text{SO}_4$  aqueous solution (2.7 wt%, 5.14 g). Then, the suspension was heated to  $100^\circ\text{C}$ , and SBA-15 (1.0 g) was added. After the same pre-carbonization process as that of OMC, a mixture of  $\beta$ -CD (0.73 g), nitrogen source (0.07 g),  $\text{H}_2\text{SO}_4$  (0.09 g), and  $\text{H}_2\text{O}$  (5 g) was added, and the suspension was similarly stirred at  $100^\circ\text{C}$  for 6 h and then heated to  $160^\circ\text{C}$  for another 6 h. The subsequent calcination and template removal procedures were also same as those of OMC. The materials using melamine, dicyandiamide, and guanidine sulfamate as nitrogen sources were, respectively, denoted as NOMC-T, NOMC-D, and NOMC-G.

The preparation of nitrogen-doped carbon material by the gel process was as follows.  $\beta$ -CD (3.0 g) and guanidine sulfamate (1.2 g) were, respectively, dissolved in  $\text{H}_2\text{SO}_4$  aqueous solution (40.0 mL, 4.8 wt%) with stirring at  $60^\circ\text{C}$  and tetraethoxysilane (6.0 g) was added. The mixed solution was kept at  $60^\circ\text{C}$  for 2 h under vigorously stirring until the TEOS was completely dissolved and then the temperature was heated to  $100^\circ\text{C}$ . After evaporation for 6 h, the mixture was increased to  $160^\circ\text{C}$  and kept at this temperature for another 6 h. The complete calcination and subsequent template removal procedures were the same as those of OMC and NOMCs. The obtained nitrogen-doped mesoporous carbon was marked as Gel-NMC.

### Characterization of materials

X-ray diffraction (XRD) patterns were collected with a Bruker D8 FOCUS X-ray diffractometer (Bruker AXS GmbH, Germany) by using  $\text{Cu K}\alpha$  radiation. The sample for TEM measurements was prepared by dropping the solution onto a copper grid, and then the grid was air-dried. The samples were examined by high-resolution TEM

with a Tecnai G2 F20 microscope, FEI, equipped with a CCD camera, Orius 832, Gatan, operating at an accelerating voltage of 200 kV.  $\text{N}_2$  adsorption and desorption experiments were performed in liquid nitrogen at 77 K by using a NOVA 2000e analyzer (Quantachrome, US). The total surface area ( $S_{\text{BET}}$ ) was calculated from the linear part of the Brunauer–Emmett–Teller (BET) curve. The pore-size distribution was determined by using the Barrett–Joyner–Halenda (BJH) method. Raman spectra were measured with a Bruker RFS 100/s Raman spectrometer with near-infrared light (1064 nm). Elemental analysis was carried out with a Vario Micro cube element analyzer. X-ray photoelectron spectroscopy (XPS) was recorded with an Axis Ultra DLD spectrometer (Kratos Analytical Ltd.) with an  $\text{Al K}\alpha$  X-ray source for excitation. The graphitic C1s band at 284.6 eV was taken as an internal standard to correct possible deviations caused by electric charging of the samples.

### Catalytic reactions

The hydrogenation of 4-nitroethylbenzene was carried out through the following route. 4-Nitroethylbenzene (0.076 g, 0.5 mmol), hydrazine hydrate (0.15 g, 3 mmol), and catalyst (0.005 g) were added into ethanol (2 mL). The reaction mixture was stirred at  $100^\circ\text{C}$  for 12 h and then analyzed by gas chromatography equipped with a 30 m RTX-wax capillary column and a flame ionization detector. In addition, the components of the products were identified by gas chromatography-mass spectrometry equipped with an HP-5 capillary column (30 m  $\times$  0.25 mm, 0.2  $\mu\text{m}$  film thickness) and an ion trap MS detector. The hydrogenations of other nitroarenes were carried out by following a similar procedure to that of 4-nitroethylbenzene.

### Acknowledgments

The work was supported by the National Nature Science Foundation of China (21432004, 21672113, and 91527301).

### Conflict of interest

The authors declare no conflict of interest.

**Keywords:** hydrogenation of nitroarenes • metal-free catalysis • ordered mesoporous carbon •  $\beta$ -cyclodextrin

- [1] a) P.-F. Zhang, J.-Y. Yuan, T. P. Fellinger, M. Antonietti, H.-R. Li, Y. Wang, *Angew. Chem. Int. Ed.* **2013**, 52, 6028–6032; *Angew. Chem.* **2013**, 125, 6144–6148; b) Y.-H. Qu, Z.-A. Zhang, X.-H. Zhang, G.-D. Ren, Y.-Q. Lai, Y.-X. Liu, J. Li, *Carbon* **2015**, 84, 399–408; c) A. Alsaiee, B. J. Smith, L.-L. Xiao, Y.-H. Ling, D. E. Helbling, W. R. Dichtel, *Nature* **2016**, 529, 190–194; d) J. Zheng, K. Wang, Y.-R. Liang, F. Zhu, D.-C. Wu, G.-F. Ouyang, *Chem. Commun.* **2016**, 6829–6832; e) H.-R. Xue, T. Wang, J.-Q. Zhao, H. Gong, J. Tang, H. Guo, X.-L. Fan, J.-P. He, *Carbon* **2016**, 104, 10–19; f) J. Wei, D.-D. Zhou, Z.-K. Sun, Y.-H. Deng, Y.-Y. Xia, D.-Y. Zhao, *Adv. Funct. Mater.* **2013**, 23, 2322–2328.
- [2] a) K. Zhou, W. Wang, Z. Zhao, G.-H. Luo, J. T. Miller, M. S. Wong, F. Wei, *ACS Catal.* **2014**, 4, 3112–3116; b) L.-M. Zhang, Z.-B. Wang, J.-J. Zhang, X.-L. Sui, L. Zhao, D.-M. Gu, *Carbon* **2015**, 93, 1050–1058.
- [3] a) X.-M. Ning, Y.-H. Li, H. Yu, F. Peng, H.-J. Wang, Y.-H. Yang, *J. Catal.* **2016**, 335, 95–104; b) S. M. Kim, Y. K. Heo, K. Bae, Y. T. Oh, M. Y. Lee, S. Y. Lee, *Carbon* **2016**, 101, 420–430; c) J.-B. Zhu, M.-L. Xiao, X. Zhao, K. Li, C.-P. Liu, W. Xing, *Chem. Commun.* **2014**, 50, 12201–12203.
- [4] a) A.-H. Lu, W.-C. Li, Z.-S. Hou, F. Schüth, *Chem. Commun.* **2007**, 1038–1040; b) B. Karimi, H. Behzadnia, M. Bostina, H. Vali, *Chem. Eur. J.* **2012**, 18, 8634–8640.

- [5] Q.-N. Wang, L. Shi, A.-H. Lu, *ChemCatChem* **2015**, *7*, 2846–2852.
- [6] a) X.-F. Guo, Y.-S. Kim, G.-J. Kim, *Catal. Today* **2010**, *150*, 22–27; b) U. G. Hong, H. W. Park, J. Lee, S. Hwang, J. Yi, I. K. Song, *Appl. Catal. A* **2012**, *415–416*, 141–148.
- [7] K. Chen, L.-H. Kang, M.-Y. Zhu, B. Dai, *Catal. Sci. Technol.* **2015**, *5*, 1035–1040.
- [8] Z.-K. Sun, B. Sun, M.-H. Qiao, J. Wei, Q. Yue, C. Wang, Y.-H. Deng, S. Kalia-guine, D.-Y. Zhao, *J. Am. Chem. Soc.* **2012**, *134*, 17653–17660.
- [9] L.-L. Li, C. Chen, L. Chen, Z.-X. Zhu, J.-L. Hu, *Environ. Sci. Technol.* **2014**, *48*, 3372–3377.
- [10] X. Wang, Y.-W. Li, *J. Mater. Chem. A* **2016**, *4*, 5247–5257.
- [11] H. Watanabe, S. Asano, S.-I. Fujita, H. Yoshida, M. Arai, *ACS Catal.* **2015**, *5*, 2886–2894.
- [12] D.-H. Guo, R. Shibuya, C. Akiba, S. Saji, T. Kondo, J. Nakamura, *Science* **2016**, *351*, 361–365.
- [13] Y.-J. Gao, G. Hu, J. Zhong, Z.-J. Shi, Y.-S. Zhu, D.-S. Su, J.-G. Wang, X.-H. Bao, D. Ma, *Angew. Chem. Int. Ed.* **2013**, *52*, 2109–2113; *Angew. Chem.* **2013**, *125*, 2163–2167.
- [14] S.-L. Yang, L. Peng, P.-P. Huang, X.-S. Wang, Y.-B. Sun, C.-Y. Cao, W.-G. Song, *Angew. Chem. Int. Ed.* **2016**, *55*, 4016–4020; *Angew. Chem.* **2016**, *128*, 4084–4088.
- [15] X.-Y. Li, X.-L. Pan, L. Yu, P. J. Ren, X. Wu, L.-T. Sun, F. Jiao, X.-H. Bao, *Nat. Commun.* **2014**, *5*, 3688–3694.
- [16] Z.-B. Zhang, Q. Zhao, J.-Y. Yuan, M. Antonietti, F.-H. Huang, *Chem. Commun.* **2014**, *50*, 2595–2597.
- [17] B. Bayatsarmadi, Y. Zheng, M. Jaroniec, S. Z. Qiao, *Chem. Asian J.* **2015**, *10*, 1546–1553.
- [18] A. Thomas, A. Fischer, F. Goettmann, M. Antonietti, J. O. Müller, R. Schlögl, J. M. Carlsson, *J. Mater. Chem.* **2008**, *18*, 4893–4908.
- [19] J. Wang, Z. Z. Wei, Y. T. Gong, S. P. Wang, D. F. Su, C. L. Han, H. R. Li, Y. Wang, *Chem. Commun.* **2015**, *51*, 12859–12862.
- [20] Y. Wang, J. S. Zhang, X. C. Wang, M. Antonietti, H. R. Li, *Angew. Chem. Int. Ed.* **2010**, *49*, 3356–3359; *Angew. Chem.* **2010**, *122*, 3428–3431.
- [21] Z. Z. Wei, J. Wang, S. J. Mao, D. F. Su, H. Y. Jin, Y. H. Wang, F. Xu, H. R. Li, Y. Wang, *ACS Catal.* **2015**, *5*, 4783–4789.
- [22] D.-Y. Zhao, J.-L. Feng, Q.-S. Huo, N. Melosh, G. H. Fredrickson, B. F. Chmelka, G. D. Stucky, *Science* **1998**, *279*, 548–552.
- [23] a) R. Ryoo, S. H. Joo, S. Jun, *J. Phys. Chem. B* **1999**, *103*, 7743–7746; b) J.-K. Hu, M. Noked, E. Gillette, Z. Gui, S. B. Lee, *Carbon* **2015**, *93*, 903–914.

Manuscript received: March 13, 2017

Revised manuscript received: April 8, 2017

Accepted manuscript online: April 12, 2017

Version of record online: May 29, 2017